Nuclear relaxation measurements in organic semiconducting polymers for application to organic spintronics

E. F. Thenell,[*] M. E. Limes,[†] E. G. Sorte,[‡] Z. V. Vardeny, and B. Saam[§]
University of Utah, Department of Physics and Astronomy, 115 South 1400 East, Salt Lake City, Utah 84112-0830, USA
(Received 10 September 2014; published 28 January 2015)

NMR measurements of spin-lattice relaxation of hydrogen nuclei in two prototype organic semiconducting solids, MEH-PPV and DOO-PPV, were carried out for temperatures between 4.2 K and room temperature, and for applied magnetic fields between 1.25 and 4.7 T. These π-conjugated polymers are of interest for use as the active semiconducting layer in spintronic devices. They typically exhibit weak spin-orbit coupling, and the interaction with inhomogeneous hyperfine fields generated by the nuclear spins plays a significant, if not dominant, role in the spin coherence and spin relaxation of electronic charge carriers. Our studies were conducted on unbiased bulk material with no photo-illumination. The characteristic ^{1}H longitudinal relaxation times in these materials ranges from hundreds of milliseconds to >1000 s, and are predominantly nonmonoexponential. We present the data both in terms of a recovery time, $T_{1/2}$, corresponding to 50% recovery of thermal magnetization from saturation and in terms of a "T_1 spectrum" produced via a numerical Laplace transform of the time-domain data. The evidence best supports relaxation to paramagnetic centers (radicals) mediated by nuclear spin diffusion as the primary mechanism: the observed relaxation is predominantly nonmonoexponential, and a characteristic T_1 minimum as a function of temperature is apparent for both materials somewhere between 77 K and room temperature. The paramagnetic centers may be somewhat-delocalized charge-carrier pairs (i.e., polarons) along the polymer backbone, although the concentration in an unbiased sample (no carrier injection) should be very low. Alternatively, the centers may be localized defects, vacancies, or impurities. Our results may also be used to judge the feasibility of Overhauser-type dynamic nuclear polarization from polarized charge carriers or optically pumped exciton states.

DOI: 10.1103/PhysRevB.91.045205 PACS number(s): 85.75.−d, 76.60.−k

I. INTRODUCTION

The inexpensive and versatile nature of π-conjugated polymer materials coupled with a rich variety of spin-mediated phenomena has made organic spintronics a rapidly growing field in semiconductor physics [1]. Such organic semiconductors (OSECs) generally exhibit weak spin-orbit coupling and correspondingly long electron-spin-coherence lifetimes, which makes them highly suitable for use in devices that rely upon the spin-dependent transport of charge carriers through an active semiconducting layer. However, exceedingly low mobility in OSECs results in spin-transport lengths in the range of tens to hundreds of nanometers [2], compared to tens of micrometers in more ordered silicon-based devices [3]. Hence, organic spintronic devices are based on thin-film active layers, generally complicating the fabrication process. Nonetheless, the relative tunability and low cost of the device materials continues to fuel further advances in the field, including the development of spin valves [4], organic light-emitting diodes (OLEDs) [5], and magnetic sensors [6].

In light of the relatively weak spin-orbit coupling, it is expected that hyperfine coupling to nuclear spins should play a significant if not dominant role in the spin relaxation of charge carriers, yet key details of how this interaction affects the magneto-transport properties of OSECs remain poorly understood. The coupling of charge carriers to the surrounding nuclear bath has major implications for spin decoherence and the associated characterization of hopping transport inside OSECs [7]. It is also possible that this coupling could result in an Overhauser-type cross polarization of the hydrogen nuclei (or of ^{13}C or deuterium in labeled materials). Enhanced nuclear polarization via techniques such as chemically induced dynamic nuclear polarization, (CIDNP) [8] and optically pumped NMR (OPNMR) [9] may also prove feasible. Of the many rate constants involved in such processes, the longitudinal relaxation time T_1 of the nuclei in OSECs is a little-studied yet important limiting parameter.

Here, we report NMR spin-lattice relaxation (T_1) measurements of hydrogen made in two prototype OSEC materials used in the fabrication of OLEDs and organic spin valves [2,10,11]: poly[2,5-dioctyloxy-1,4-phenylene-vinylene] (DOO-PPV) and poly[2-methoxy-5-(2-ethylhexyloxy)-p-phenylene vinylene] (MEH-PPV) (see Fig. 1). These initial experiments were done on bulk material, with no electrical or photoexcitation. We found that the characteristic values of T_1 vary widely, from hundreds of milliseconds to thousands of seconds, depending on applied magnetic field and temperature. Additionally, we found that the relaxation behavior in many instances is significantly nonmonoexponetial, leading us to conclude that spin diffusion to paramagnetic centers is likely the dominant relaxation mechanism. These centers are likely to be material paramagnetic impurities (e.g., vacancies or dangling bonds). They could also be localized charge carriers responsible for the conducting behavior in OSP devices; however, we find this to be less likely in our bulk samples, where without the

[*]ethenell@gmail.com
[†]Present address: Department of Physics, Princeton University, Princeton, New Jersey 08544, USA.
[‡]Present address: Department of Chemistry, Georgetown University, Washington, DC 20057, USA.
[§]saam@physics.utah.edu

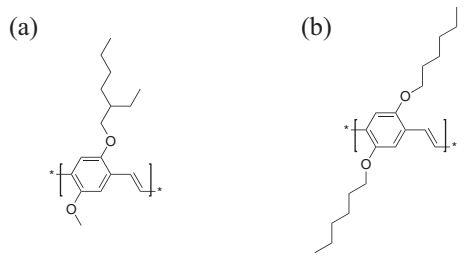

FIG. 1. Molecular structures for (a) MEH-PPV (260.18 Da per monomer) and (b) DOO-PPV (358 Da per monomer). Bond lengths vary between 0.1 and 0.15 nm, but the disordered packing behavior of the long polymer chains can cause spacing between adjacent chains to be much larger.

requisite photoexcitation or charge injection such carriers exist only in very low concentrations. Given this complexity and following Fukushima and Uehling [12], we recorded $T_{1/2}$, the time for an initially unpolarized sample to return to half of its equilibrium value; the results for various applied magnetic fields and temperatures are shown in Table I. We note here that our T_1 measurements are all of this "saturation-recovery" variety. In Sec. III, we provide a more detailed characterization of the relaxation curves with a Laplace-transform approach, which shows the relative intensities of different exponential components in each case.

II. THEORY

In broad terms, the possible relaxation mechanisms for spin-$\frac{1}{2}$ nuclei, for which there can only be magnetic (i.e., no quadrupolar) interactions, in an OSEC are relatively limited. Nuclei in semiconducting materials are generally subject to relaxation via interactions with thermally generated (unpaired-spin) charge carriers in the conduction band [13,14]. However, this mechanism is utterly negligible in undoped conventional semiconductors, where the equilibrium density of charge carriers is on order 10^{12} to 10^{13} cm^3. The band gap in OSEC materials is $\approx$2 eV; large enough that, even at room temperature, the equilibrium concentration of charge carriers should be similarly small. (We return later to the question of the nature and density of charge carriers in OSECs in connection with the mechanism of relaxation to paramagnetic centers.) Another known mechanism is the spin-rotation coupling between moving electrons and the nucleus, modulated by Raman phonon scattering [15,16]. This mechanism is particularly weak for low-Z materials (it has been studied, for example, in solid ^{129}Xe [17] and ^{207}Pb salts [18]) and at low temperatures, where phonons are frozen out. Indeed, there is a characteristic quadratic dependence (as per phonon occupation number) of $1/T_1$ on temperature, which is not observed anywhere in our data. The nuclear dipole-dipole interaction, modulated by molecular motions, can also be a source of relaxation. These motions are not necessarily frozen out at low temperatures in disordered polymer materials. Indeed, such a mechanism has been identified [19,20] as a dominant source of T_1 relaxation in organic polymer materials consisting of much smaller molecules than MEH-PPV and DOO-PPV. Bloise *et al.* [21] used ^{13}C NMR to study molecular motion in MEH-PPV. With one exception (discussed in Sec. IV) the motions occur on timescales that are too long to effectively mediate nuclear dipole-dipole relaxation. This leaves the interaction of nuclear spins with paramagnetic centers (radicals) as the only other known mechanism. Nuclear spins closer to these centers can undergo direct dipole-dipole cross relaxation, leading to polarization gradients along which spin angular momentum from more distant spins can flow diffusively. Such spin diffusion is mediated by mutual spin flips among nearest-neighbor nuclei, which occur on the timescale of the nuclear spin T_2 [22]. This relaxation mechanism has been observed in both insulating [12,23] and semiconducting [24] solid-state systems and is characterized by the equation [12,22]

$$\dot{M}(r,t) = D\nabla^2 M(r,t) - \frac{C}{r^6} M(r,t), \tag{1}$$

where M is the fractional magnetization difference from equilibrium magnetization, D is the spin-diffusion coefficient, and C is the dipolar-coupling coefficient. An angular dependence in C, arising from the orientation of the applied field B_0 relative to the line connecting the paramagnetic center to the nucleus, can usually be averaged away for a polycrystalline or disordered sample, so that one obtains [25]

$$\bar{C} = \frac{2}{5}(\hbar\gamma_S\gamma_I)^2 S(S+1)\left[\frac{\tau_c}{1+\omega_I^2\tau_c^2}\right], \tag{2}$$

where S and I refer respectively to the spins of the paramagnetic center and of the nucleus, γ is the gyromagnetic ratio, $\omega_I = \gamma_I B_0$ is the nuclear Larmor frequency, and τ_c is the correlation time for the interaction, taken here to be the longitudinal relaxation time of the paramagnetic center.

TABLE I. Values of $T_{1/2}$, in seconds, for ^{1}H in the organic semiconducting polymers MEH-PPV and DOO-PPV as a function of applied magnetic field and temperature. The parameter $T_{1/2}$ is the time for recovery of magnetization from an initially unpolarized state to half of its thermal-equilibrium value. Values shown in the "$\sim$150 K" row were taken at temperatures near 150 K, where the temperature drift as the cryostat warmed to room temperature from 77 K was slowest. (Specific values for each measurement are given in Fig. 3.)

DOO-PPV			
	4.7 T	2.5 T	1.25 T
4 K	1130 ± 35	3.75 ± 0.10	15 ± 1
10 K	225 ± 10	0.70 ± 0.04	6.3 ± 0.2
50 K	4.1 ± 0.1	8.4 ± 0.4	
77 K	4.4 ± 0.1	2.4 ± 0.1	1.52 ± 0.06
$\sim$150 K	0.29 ± 0.01	0.165 ± 0.005	
291 K	0.44 ± 0.02	0.260 ± 0.005	
MEH-PPV			
	4.7 T	2.5 T	1.25 T
4 K	9.0 ± 0.5	37.5 ± 4.5	16.3 ± 0.4
10 K	50 ± 2	8.6 ± 0.7	0.45 ± 0.10
50 K	15.0 ± 0.5	4.0 ± 0.2	
77 K	1.40 ± 0.25	1.5 ± 0.1	
$\sim$150 K	0.29 ± 0.01	0.24 ± 0.01	
291 K	0.34 ± 0.01	0.25 ± 0.01	

Equation (1) is not generally solvable analytically. Limiting regimes have been identified [23,26,27], under the assumption that the paramagnetic centers are dilute enough that each nucleus is affected by only one such center, by comparing two characteristic distances. Within the diffusion-barrier radius b, one assumes that the local field surrounding each nucleus is so strongly shifted by the presence of the nearby paramagnetic center that it is completely removed from the magnetic resonance line and cannot be detected by NMR. Furthermore, nuclei within the diffusion-barrier radius cannot exchange energy with nuclei outside the barrier radius via mutual spin flips. In the case where the nuclear spin $T_2 \gg \tau_c$, we can estimate b by comparing the thermal-equilibrium ensemble magnetic moment $\mu_S[\mu_S B_0/(kT)]$ of the paramagnetic centers to μ_I [23]:

$$b = a\left(\frac{\mu_S^2 B_0}{\mu_I kT}\right)^{1/3}, \tag{3}$$

where a is the lattice parameter, k is the Boltzmann constant, and T is absolute temperature. The other characteristic distance in the problem is the pseudopotential radius ρ, roughly the maximum distance from a given paramagnetic center at which the center can relax nuclei through the direct dipole-dipole interaction described by Eq. (2). It can be expressed as [12]

$$\rho = 0.68\left(\frac{C}{D}\right)^{1/4}. \tag{4}$$

In the "fast-diffusion" regime of $\rho \ll b$, relaxation is limited by $1/\tau_c$, the rate at which the paramagnetic centers leak angular momentum to the lattice. In this regime, spin diffusion is rapid enough to equilibrate the sample on timescales short compared to the relaxation time, and the sample is well characterized at all times by a single spin temperature. As a result, one expects monoexponential behavior to characterize the entire approach to equilibrium from an initial unpolarized state with a characteristic rate is given by [23]

$$\frac{1}{T_{1f}} = \frac{4\pi}{3}\frac{NC}{b^3}, \tag{5}$$

where N is the concentration of paramagnetic centers. In the "diffusion-limited" regime, $\rho \gg b$, diffusion is slow enough that significant gradients in the polarization develop during the approach to equilibrium. The presence of such gradients means that the sample cannot be described by a single spin temperature, and the corresponding spin-lattice relaxation exhibits multiexponential behavior corresponding to the multimode spin diffusion given by Eq. (1). The late-time rate (slowest diffusion mode) is given by [26,27]

$$\frac{1}{T_{1s}} = \frac{17}{2}NC^{1/4}D^{1/4}, \tag{6}$$

where we emphasize that Eqs. (5) and (6) are valid in the low-concentration limit, i.e., $\rho \ll R$, where R is the mean distance between paramagnetic centers. Fukushima and Uehling [12] treat the more general case of larger values of N. For some very short time t, spin diffusion cannot occur because significant polarization gradients have not yet developed in the sample. Blumberg [23] first formulated the expression for magnetization recovery in this regime:

$$M(t) = 1 - (4/3)\pi^{3/2}NC^{1/2}t^{1/2}, \tag{7}$$

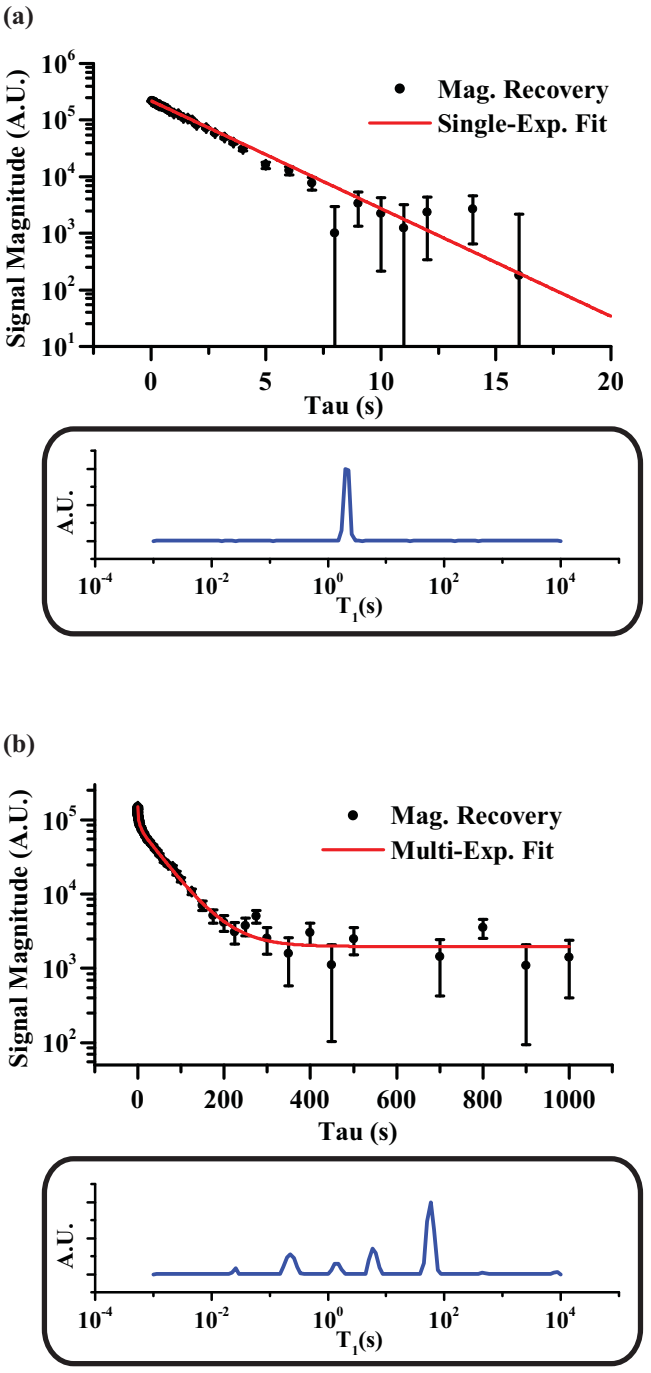

FIG. 2. (Color online) (a) Magnetization recovery of ^{1}H vs time in DOO-PPV at 1.25 T and 77 K. This is a relatively rare instance in these measurements where the decay fits reasonably well to a single exponential. The boxed graph shows corresponding Laplace transform having a single peak corresponding to $T_1 = 2.28 \pm 0.04$ s (uncertainty extracted from the fit to the time-domain data). (b) Magnetization recovery of ^{1}H vs time in MEH-PPV at 2.5 T and 10 K. Here, the decay is strongly nonmonoexponential. The boxed graph shows corresponding Laplace transform which shows many peaks, some of which are not reflected in the multiexponential fit to the time-domain data.

which is valid for $t < C^{1/2}D^{-3/2}$ or, equivalently, when the characteristic spin-diffusion distance is shorter than the characteristic distance over which the dipolar field from the paramagnetic center falls off. The $t^{1/2}$ dependence might be considered an indicator for the impurity-relaxation mechanism; however, such a dependence is not easily distinguishable from a simple exponential dependence over the range of times for which it is supposed to be valid [12]. Moreover, in saturation-recovery experiments, the earliest time points have the lowest signal-to-noise ratio (SNR).

The magnetic-decoupling factor in square brackets in Eq. (2) gives rise in the usual way [28] in both regimes to a minimum T_1 value when $\omega_I \tau_c = 1$, i.e., when the Larmor period is equal to the relaxation time of the paramagnetic center. Thus, in the high-field limit $\omega_I \tau_c \gg 1$, $T_1 \propto B_0^2$ in the fast-diffusion regime and $T_1 \propto B_0^{1/2}$ in the diffusion-limited regime. In principle, transitions between these regimes can thus be studied by measuring T_1 as a function of temperature and applied field.

Beyond simply recording the $T_{1/2}$ times in Table I, we provide a more general characterization of longitudinal relaxation for these materials by implementing a Laplace-transformation scheme to an effective T_1 space. The general form of the Laplace transform is

$$F(s) = \int_0^\infty e^{-st} f(t)\, dt. \tag{8}$$

Now, if we let $f(t)$ represent the recovery of the sample magnetization as a function of time toward its thermal equilibrium value from $f(0) = 0$, and $s = 1/T_1$, we obtain a spectrum of T_1 values from the time-domain relaxation data $f(t)$. Representative time-domain data and corresponding T_1 spectra are shown in Fig. 2(a) for monoexponential and in Fig. 2(b) for multiexponential decays.

III. EXPERIMENT

MEH-PPV was purchased as product number ADS100RE (American Dye Source). DOO-PPV was synthesized in house. Both of these materials were ground into a powder, then stored in 2-cm-long by 5-mm-diameter pyrex cylindrical NMR sample containers, sealed with teflon plugs. Pulsed-NMR experiments were performed on the DOO-PPV sample over the course of two years, whereas the experiments performed on the MEH-PPV sample spanned six months. The sealed sample containers helped to slow effects of degradation due to oxygen exposure.

All data were acquired with a Redstone (Tecmag) NMR spectrometer and various homebuilt tunable probes with 50 Ω impedance, resonant at the Larmor frequency $\omega_0 = \gamma_p B_0$, where the ^{1}H gyromagnetic ratio $\gamma_p = 2\pi(42.58\ \text{MHz})/\text{T}$, and the values of B_0 were 4.7, 2.5, and 1.25 T (see Table I). A conventional capacitively tapped probe design was used at 21 and 53 MHz, and a high-frequency design [29] was used at 85 and 200 MHz. The rf power amplifier, model BT-02000-AlphaSA-T (Tomco), operated between 20 and 500 W (1% to 25% of maximum output power). The longitudinal relaxation time T_1 of ^{1}H in MEH-PPV and DOO-PPV was measured by using the saturation-recovery method: an initial series of hard pulses to destroy any longitudinal magnetization, a variable wait time τ, and a final read pulse to project some fixed fraction of the recovered magnetization into the transverse plane and record the intensity of the resulting free-induction decay (FID). The saturation comb consisted of ten to fifty 1 μs pulses separated by a time $T_2 \ll t_{\text{sep}} \ll T_1$, typically ≈5 ms. In general, the saturation comb preceded each time point in a T_1 measurement and was followed by a $\pi/2$ read pulse to maximize the signal from the recovered magnetization. However, in some cases where the SNR allowed, the saturation comb was implemented once at the beginning of the entire T_1 measurement, and a low-flip-angle ($<1^\circ$) read pulse was used at successive time points in the recovery, significantly decreasing measurement time for many of the longer-T_1 measurements.

All experiments were performed in a vertical wide-bore (89 mm) superconducting magnet (Oxford), for which the field was adjusted down from its maximum (8.0 T) to each of the three measurement fields listed in Table I, and in a model MD3A variable-temperature cryostat (Oxford) designed to fit inside the magnet bore. A Cernox (Lakeshore) temperature sensor mounted at the dewar's heat exchanger was used to monitor and control the temperature between 4 and 77 K. For measurements 77 K and higher the dewar was first cooled to 77 K and then allowed to drift slowly back toward room temperature. This drift could be maintained $\leqslant$0.1 K/min and never exceeded a total of 2 K over the course of a T_1 measurement. Each measurement was taken twice, at minimum, to ensure that the observed exponential components were consistent and reproducible.

Results across the accessible values of applied field and temperature are shown for both MEH-PPV and DOO-PPV in Fig. 3. For the highest temperatures and lowest applied fields, the large dipolar linewidth (corresponding to $T_2 \lesssim 20\ \mu$s) led to a relatively low SNR, which precluded reliable measurement of T_1. In most cases, the time-domain data are highly nonmonoexponential. For better characterization of these data, we implemented the CONTIN algorithm [30] for a numerical discrete Laplace transformation to a normalized relaxation spectrum, where the intensity at each value of time on the horizontal axis indicates the relative weight of that T_1 component in an assumed multiexponential decay. We note that the uniform width of the spectral peaks is related to finite sampling and does not appear to carry any physical significance. A similar width is generated from the transform of an ideal monoexponential decay and shows no appreciable dependence on artificially added noise. We treat the transformed data as only a number and intensity of discrete characteristic decay times because we are unable to distinguish any further complexity in the spectral characteristics.

IV. RESULTS AND DISCUSSION

In general, with lower temperature and increased magnetic field strength, longitudinal relaxation of ^{1}H in MEH-PPV and DOO-PPV becomes both longer and more highly nonmonoexponential, ranging from over 1000 s for DOO-PPV at 4 K and 4.7 T to a few hundred milliseconds for both materials at 150 K and above. Low SNR precluded data acquisition for $T \gtrsim 77$ K at 1.25 T, but the trends in our data indicate that relaxation times in this regime would be on the order of

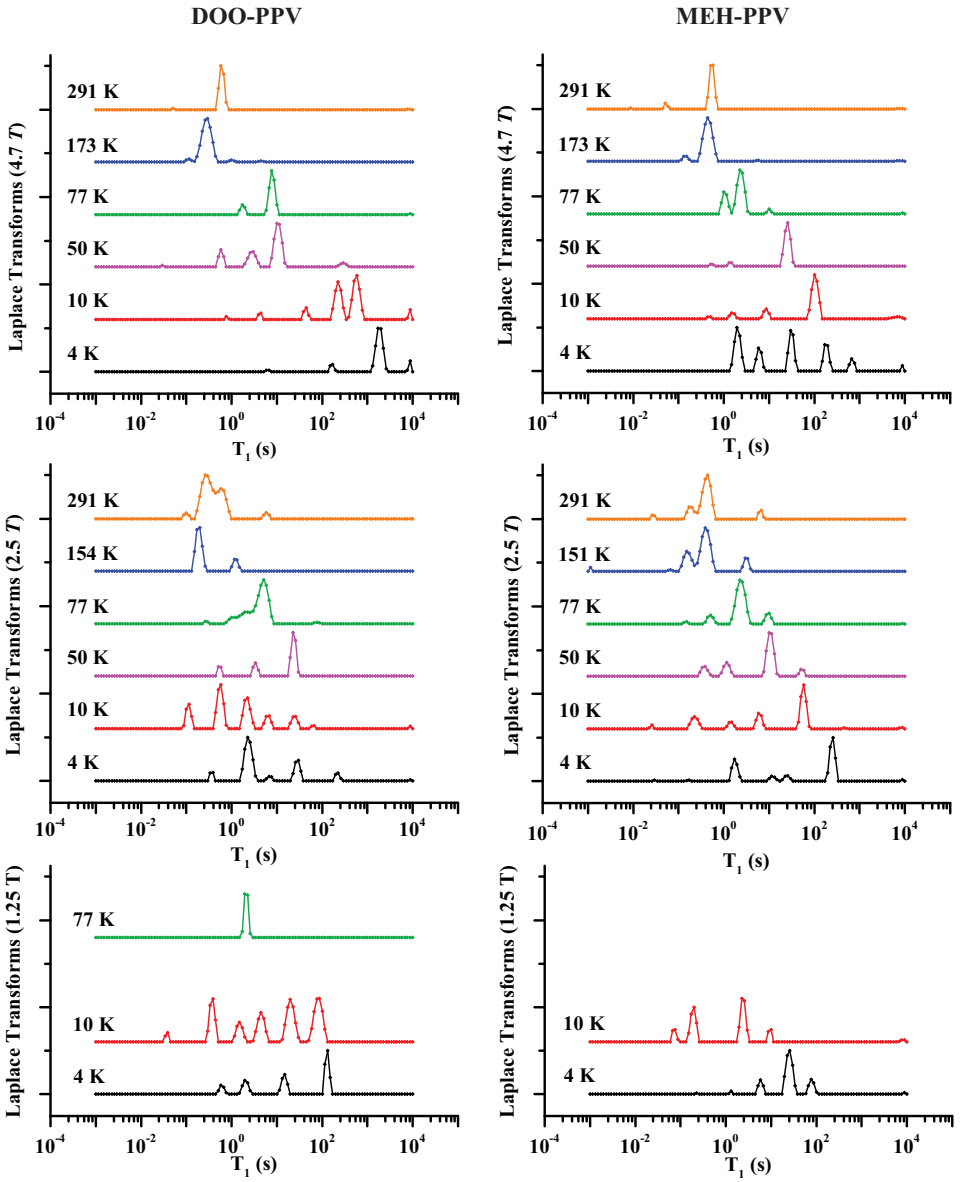

FIG. 3. (Color online) The relaxation spectrum for ^{1}H in DOO-PPV and MEH-PPV as determined by taking the Laplace transform of time-domain saturation-recovery data. If one assumes a multiexponential decay model, then the intensities correspond to the weights of the various T_1 components. Nonmonoexponential behavior, in general, tends to be most prevalent at lowest temperatures and highest fields. Significant dependence of the relaxation behavior on both temperature and magnetic field is observed; the largest T_1 component may pass through an apparent minimum between 77 K and room temperature.

100 ms and relatively monoexponential. In comparing the two materials, DOO-PPV has significantly longer relaxation times at the highest field measured, but this property disappears or is even reversed somewhat at lower applied fields.

Whether we approach the diffusion-limited or the fast-diffusion regimes described in Sec. II depends on our limited knowledge of quantities such as the spin-diffusion coefficient D, the dipolar coupling coefficient $\bar{C}$ (via the correlation time τ_c), and the concentration N of paramagnetic centers. From Eq. (2), we find $\bar{C} \approx 7 \times 10^{-32}$ cm^6/s for $\tau_c = 1$ ns. (The rationale for choosing $\tau_c \approx 1$ ns comes from the observed T_1 minimum, as discussed at length below.) Even if the diffusion coefficient is assumed to have a large range from 10^{-12} cm^2/s to as low as 10^{-16} cm^2/s, the range for the pseudopotential radius in Eq. (4) is about 1 to 10 nm. For longer τ_c or larger B_0, this range decreases as $\tau_c^{-1/2}$. From Eq. (3), we calculate a range for the barrier radius b of about 1 to 10 lattice constants, where the higher end of that range corresponds to $B_0 = 4.7$ T and $T = 4$ K. If we take a to correspond to typical bond lengths of 1 to 1.5 Å, we see that we cannot reasonably assume a significant separation in length scales for ρ and b. Additionally, if we assume the diffusion-limited regime, we can calculate N from Eq. (6) for reasonable values of $D = 10^{-14}$ cm^2/s, $\tau_c = 1$ ns, and $T_1 = 1$ s, obtaining $N = 4 \times 10^{12}$ cm^{-3}. On the other hand, assuming the slow-diffusion regime with $b = 10^{-7}$ cm, $\tau_c = 1$ ns, and $T_1 = 1$ s yields $N = 3 \times 10^{18}$ cm^{-3}. These are almost certainly extreme values for N, with the actual number likely lying somewhere between the more reasonable

values of 10^{14} cm^{-3} and 10^{16} cm^{-3}. These calculations lead us to conclude that our experimental parameters lie between the fast-diffusion and the diffusion-limited regimes.

Although Eq. (1) cannot be solved analytically in this intermediate regime, our essential hypothesis of proton relaxation (with associated spin diffusion) to paramagnetic centers is supported by two key features of the data shown in Fig. 3. First, we observe predominantly nonmonoexponential relaxation across most values of field and temperature—a signature of the nonuniform spin temperature resulting from spin diffusion towards discrete localized centers of relaxation in the bulk material. In fact, there is considerable evidence in the literature to suggest that paramagnetic centers of several varieties could be present in OSECs. Materials such as DOO-PPV and MEH-PPV are of interest for organic spintronics precisely because lattice impurities create trapped electronic states between the HOMO and LUMO bands. The existence of these states allows for the generation of precursor polaron pair states, upon which spin-dependent transport properties of organic spintronic devices depend sensitively [31,32]. Since in this work we studied these materials with no applied bias or illumination, such carriers may still exist in our samples but in much lower concentration. Other fixed paramagnetic centers can result from defects, vacancies, or dangling bonds that are not necessarily associated with conduction in the π-conjugated chain, all of which are known to exist in significant densities in π-conjugated semiconducting polymers [33]. Whether charge carriers in such localized precursor-pair states are some significant fraction of the paramagnetic centers responsible for ^{1}H T_1 relaxation in these materials remains an open question that might be addressed through similar T_1 measurements performed with samples under illumination to generate such pairs. From the standpoint of nuclear relaxation, localized or only slightly delocalized charge carriers would produce the same basic relaxation characteristics in the solid as ordinary paramagnetic centers in insulating materials [13].

A second key feature of the data is an apparent minimum value in T_1 (considering either the $T_{1/2}$ values in Table I or the dominant peaks in the T_1 spectra of Fig. 3) somewhere between 77 K and room temperature for both of the higher applied fields of 2.5 and 4.7 T. Regardless of how close the system is to either limiting regime of spin diffusion in Eq. (1), the theory predicts such a minimum to occur for $\omega_I^2\tau_c^2 \approx 1$, from which we can extract an associated correlation time of $\tau_c = 1$ to 2 ns. While electron spin-relaxation times in solids vary widely according to material, temperature, and applied field [34], this is a reasonable timescale for relaxation of paramagnetic centers in paramagnetic salts [35,36], bulk inorganic semiconductors [37], and glasses doped with iron oxides [38], particularly at 77 K and above [39]. We note here that our extracted value of τ_c is much shorter than timescales reported by Baker *et al.* [7] ($\gtrsim$36 μs) in their study of spin dephasing of polaron pairs in MEH-PPV at room temperature, where coherence times (ultimately limited by the polaron T_1) can be quite long. However, as discussed above, polarons exist in negligible concentrations in bulk OSECs without photo excitation or charge injection, so it is unlikely that such states are relevant for the nuclear spin relaxation observed here. More generally, the weaker spin-orbit coupling in organic materials would argue for longer values of τ_c than those observed in typical high-Z inorganic materials, as the prevalent relaxation mechanisms generally have to do with direct or indirect (Raman) phonon processes that modulate the spin-orbit interaction. In any case, we would generally expect τ_c to decrease with temperature and, thus, for the longest T_1 values to be measured at the highest applied fields and lowest temperatures ($\omega_I^2\tau_c^2 \gg 1$).

It is important to note that motion of the spins inside the bulk solid could produce effects analogous to the T_1-minimum effects discussed previously. In fact, studies of motion in some organic systems show signs of significant motion even at temperatures as low as 4 K [19,20]. However, Bloise *et al.* [21] showed that, although the macromolecules do go through small-angle rotations in the solid state, the timescales for this motion are on order 100 ms, far too slow to play a significant role in nuclear spin relation at these magnetic fields. However, Bloise *et al.* do observe free rotations of the terminal CH_3 groups on the polymer side chains that have thermal activation energies in the 0.06 to 0.1 eV range. Although these activation energies exclude the possibility of this motion playing a role in nuclear-spin relaxation at low temperatures, these motions may not be completely frozen out close to room temperature. In regimes where the motion is present, it has a correlation time on order 1 to 10 ns and therefore can produce fluctuations in the local magnetic fields with frequency on the order of ω_I. Since this motion would be possible in all terminal CH_3 groups in all polymer chains, any relaxation of nuclear spins associated with this mechanism would be uniform across the sample and would therefore suppress nonmonoexponential relaxation behavior once the motion is thermally activated. Since this suppression appears to have a more pronounced effect at 4.7 T than at 2.5 T, it is likely that the local field fluctuations caused by this motion have a frequency $>$100 MHz.

The distribution of chain lengths and the strongly disordered packing of the chains in these materials plays a critical role in any relaxation mechanism that depends on spin diffusion. The strong dipolar coupling of nearby ^{1}H nuclei in both of these materials leads to a large dipolar linewidth, corresponding to $T_2 \lesssim 20$ μs, where we note that the receiver dead time (5 to 10 μs) precludes a more precise characterization of the transverse relaxation and NMR spectrum. This strong coupling would lead to a large spin-diffusion coefficient: using Bloembergen's original estimate of $D \sim a^2/(50T_2)$, we calculate $D \approx 1 \times 10^{-13}$ cm^2/s by using the reasonable values of $a = 0.1$ nm and $T_2 = 20$ μs. However this would apply only to protons along a single polymer chain and perhaps to places where protons on separate chains happen to lie close enough together for dipolar coupling to be important. The DOO-PPV sample was synthesized with a nominal target value of 20 monomers per chain, whereas the nominal value for the MEH-PPV sample is $>$380. In both cases, the concentration of paramagnetic centers is almost certainly much less than one per chain, and effective relaxation by spin diffusion must therefore include hopping from chain to chain. Such hopping is likely to be characterized by a much smaller diffusion coefficient than calculated above. Multimode diffusion with at least two very different diffusion coefficients, even within either analytically describable limiting regime, likely leads to a complicated T_1 spectrum that is difficult to interpret in terms of matching

the behavior of particular relaxation components to the theory presented in Sec. II.

One might invoke the shorter DOO-PPV polymerization length to account for the significant difference in T_1 between the two materials at high field and low temperature: given comparable densities of paramagnetic centers in a regime where spin diffusion plays an important role in relaxation, there could be a bottleneck in flipping spins between shorter chains, i.e., the DOO-PPV sample would have a longer T_1 because the characteristic spin-diffusion coefficient for interchain flips is much smaller than that for intrachain flips. While this represents a plausible explanation for the observed behavior at 4.7 T, it does not account for the reversal of the identified trend at 2.5 T (slower relaxation in MEH-PPV), although the rate increases dramatically (by more than two orders of magnitude) for DOO-PPV in going from 4.7 to 2.5 T at 4 K. Indeed, the 2.5 T values measured for DOO-PPV at 4 and 10 K stand apart by being so large compared to all other data for both materials.

V. CONCLUSION

We presented a systematic study of proton spin-lattice relaxation times in two widely studied OSECs as a function of both temperature and applied magnetic field. These measurements identified nuclear spin diffusion to paramagnetic impurities as a dominant relaxation mechanism in these solids, which produces the multiexponential relaxation behavior observed in many of our measurements. To analyze this multiexponential relaxation behavior, we implemented a Laplace transform algorithm to transform relaxation measurements into T_1 spectra, which are plotted as a function of temperature and magnetic field strength. Thus, although our experimental parameters place our system of study somewhere between the two most common analytically solvable regimes of Eq. (1), our hypothesis of diffusion to paramagnetic centers as the dominant relaxation mechanism in OSECs is supported by (1) our observation of nonmonoexponential relaxation behavior across a range of temperatures and magnetic fields and (2) the identification of a T_1 minimum value which gives a reasonable estimate of the lifetime of the trapped electronic states likely serving as the paramagnetic centers of relaxation in these materials. In addition to identifying a likely mechanism for nuclear spin relaxation in OSECs, knowledge of nuclear T_1 values could prove helpful as attempts to hyperpolarize nuclei in OSECs through dynamic nuclear polarization (DNP) methods such as CIDNP or OPNMR continue. Since our data show nuclear T_1s to be much longer than the lifetimes of typical electronic spin states in OSECs, it is unlikely to be a limiting factor in any such experiment.

ACKNOWLEDGMENTS

We acknowledge helpful discussions with K. van Schooten, A. Thiessen, and C. Boehme. We are also grateful to L. Wojcik for synthesizing the DOO-PPV. This work was supported by the NSF Materials Research Science and Engineering Center (MRSEC) at the University of Utah (Grant No. DMR11-21252), as well as by NSF Grant No. DMR-1104495.

[1] *Organic Spintronics*, edited by Z. V. Vardeny (CRC Press, Boca Raton, FL, 2010).
[2] T. D. Nguyen *et al.*, Nat. Mater. **9**, 345 (2010).
[3] I. Appelbaum, B. Huang, and D. J. Monsma, Nature (London) **447**, 295 (2007).
[4] Z. H. Xiong, D. Wu, Z. V. Vardeny, and J. Shi, Nature (London) **427**, 821 (2004).
[5] T. D. Nguyen, E. Ehrenfreund, and Z. V. Vardeny, Science **337**, 204 (2012).
[6] W. J. Baker *et al.*, Nat. Commun. **3**, 898 (2012).
[7] W. J. Baker, T. L. Keevers, J. M. Lupton, D. R. McCamey, and C. Boehme, Phys. Rev. Lett. **108**, 267601 (2012).
[8] E. Daviso, G. Jeschke, and J. Matysik, in *Biophysical Techniques in Photosynthesis II*, edited by T. J. Aartsma and J. Matysik (Springer, Dordrecht, 2008), p. 385.
[9] S. E. Barrett, R. Tycko, L. N. Pfeiffer, and K. W. West, Phys. Rev. Lett. **72**, 1368 (1994).
[10] D. R. McCamey, S. Y. Lee, S. Y. Paik, J. M. Lupton, and C. Boehme, Phys. Rev. B **82**, 125206 (2010).
[11] S.-Y. Lee *et al.*, J. Am. Chem. Soc. **133**, 072019 (2011).
[12] E. Fukushima and E. A. Uehling, Phys. Rev. **173**, 366 (1968).
[13] N. Bloembergen, Physica **20**, 1130 (1954).
[14] A. Abragam, *Principles of Nuclear Magnetism* (Oxford University Press, Oxford, 1961), p. 389.
[15] R. J. Fitzgerald, M. Gatzke, D. C. Fox, G. D. Cates, and W. Happer, Phys. Rev. B **59**, 8795 (1999).
[16] A. J. Vega, P. A. Beckmann, S. Bai, and C. Dybowski, Phys. Rev. B **74**, 214420 (2006).
[17] N. N. Kuzma, B. Patton, K. Raman, and W. Happer, Phys. Rev. Lett. **88**, 147602 (2002).
[18] P. A. Beckmann, S. Bai, A. J. Vega, and C. Dybowski, Phys. Rev. B **74**, 214421 (2006).
[19] S. Voelker *et al.*, J. Chem. Phys. **67**, 1759 (1977).
[20] J. Friedrich and D. Haarer, Angew. Chem., Int. Ed. Engl. **23**, 113 (1984).
[21] A. C. Bloise, E. R. deAzevedo, R. F. Cossiello, R. F. Bianchi, D. T. Balogh, R. M. Faria, T. D. Z. Atvars, and T. J. Bonagamba, Phys. Rev. B **71**, 174202 (2005).
[22] N. Bloembergen, Physica **15**, 386 (1949).
[23] W. E. Blumberg, Phys. Rev. **119**, 79 (1960).
[24] A. M. Panich, C. L. Teske, and W. Bensch, Phys. Rev. B **73**, 115209 (2006).
[25] A. Abragam, *Principles of Nuclear Magnetism* (Oxford University Press, Oxford, 1961), p. 380.
[26] P.-G. de Gennes, J. Phys. Chem. Solids **7**, 345 (1958).
[27] G. R. Khutsishvili, Sov. Phys. Usp. **11**, 802 (1969).
[28] E. Fukushima and S. B. W. Roeder, *Experimental Pulse NMR: A Nuts and Bolts Approach* (Addison-Wesley, Reading, MA, 1981), p. 141.
[29] D. D. Wheeler and M. S. Conradi, Concepts Magn. Reson., Part A **40A**, 1 (2012).
[30] S. W. Provencher, Comput. Phys. Commun. **27**, 229 (1982).

[31] H. Meyer, D. Haarer, H. Naarmann, and H. H. Horhold, Phys. Rev. B **52**, 2587 (1995).
[32] J. Behrends, K. Lips, and C. Boehme, Phys. Rev. B **80**, 045207 (2009).
[33] A. Moliton and R. C. Horns, Polym. Int. **53**, 1397 (2004).
[34] R. Lopez, in *Computational and Instrumental Methods in EPR*, edited by C. Bender and L. J. Berliner (Springer, United States, 2007), pp. 31–82.
[35] G. Ablart and J. Pescia, Phys. Rev. B **22**, 1150 (1980).
[36] M. Nogatchewsky, G. Ablart, and J. Pescia, Solid State Commun. **24**, 493 (1977).
[37] T. F. Boggess, J. T. Olesberg, C. Yu, M. E. Flatte, and W. H. Lau, Appl. Phys. Lett. **77**, 1333 (2000).
[38] T. Bouhacina, G. Ablart, J. Pescia, and Y. Servant, Solid State Commun. **78**, 573 (1991).
[39] J. S. Colton, M. E. Heeb, P. Schroeder, A. Stokes, L. R. Wienkes, and A. S. Bracker, Phys. Rev. B **75**, 205201 (2007).